



Experimental Investigations on Mechanical and Wear Behaviour of 2014Al–Al₂O₃ Composites

V. Bharath¹ · V. Auradi¹ · Madeva Nagara² · Satish Babu Boppana³

Received: 2 January 2020 / Revised: 10 February 2020 / Accepted: 18 February 2020 / Published online: 3 March 2020
© Springer Nature Switzerland AG 2020

Abstract

In the existing exploration, an effort is being made to synthesize Al₂O_{3p} ceramic-reinforced 2014Al matrix composites by liquid stirring (Stir Casting) in order to contemplate the effect of Al₂O_{3p} on mechanical and wear properties of the prepared composites. The Al₂O_{3p} ceramic additional level is maintained at 9, 12 and 15 wt%. An innovative method of adding 2-stage reinforcements during liquid stirring is used throughout the course of preparation of each composite. An average particle size of 53 μm Al₂O_{3p} is used. By using scanning electron microscopy (SEM), microstructural characterization is performed for the above synthesized composites, which showed moderately uniform Al₂O_{3p} distribution with matrix grain refinement accompanied by X-Ray Diffraction (XRD) analysis. The hardness of the resultant composites is examined using Zwick micro hardness tester and the above synthesized composites are examined mechanically as per ASTM standards by means of computerized universal testing machine. With increment in wt% of Al₂O_{3p}, improvements in the value of hardness and tensile strength of the synthesized composites were seen. Percentage improvements of 28.88% (9 wt%), 43.36% (12 wt%) and 68.54% (15 wt%) in terms of hardness and 5.09% (9 wt%), 17.62% (12 wt%) and 29.03% (15 wt%) in terms of tensile strength were obtained, respectively. The sliding wear test is carried out by using a computerized pin on a disc wear tester with counter surface as an EN31 steel disc (HRC60) and composite pin as specimens. The synthesized composites revealed the superior wear resistance property. Worn surfaces were studied with the help of SEM in order to know the wear mechanism. Overall investigation outcomes are very interesting and motivate to carry out further research work.

Keywords 2014Al alloy · Al₂O_{3p} · Ceramics · Liquid stirring · Hardness · Wear

1 Introduction

Aluminium matrix composites (AMC's) are becoming to be a plainly potential engineering material that offers a good combination of properties, parenthetically: high specific strength and stiffness, good thermal conduction and good electrical conduction. Due to good combinations of properties along with light weight, AMC's are growing as advanced materials for a couple of applications in aviation, defence and automotive; these promising new materials have

been discovered in the present years and the types of uses in vehicles reminiscent of the ultimate goal of improving the fuel capacity have been analysed in depth. AMC's are certain to be paired with a number of supporting items in the various product categories, particularly in cylindrical blocks and liners, driver shaft etc. In aviation sectors, aluminium composites are utilised primarily in structural applications, for example, aero vehicle body components, drive shafts, engine and rotor vanes in compressors [1–4]. Such sector implementation is based entirely on the importance of their wear characteristics.

As of now, thought is being paid to the usage of good quality Al–Al₂O_{3p} composites for elementary applications in aviation and general outlining regions so far [5]. Hassan et al. [6] discovered that the wear and tear loss of the copper-containing composites is smaller compared to copper-free composites. Kok and Ozdin [7] in their examinations on 2024Al–Al₂O_{3p} composites surveyed the impact of the addition of Al₂O_{3p} and its size on the wear and tear conduct

✉ V. Bharath
bharathv88@gmail.com

¹ Siddaganga Institute of Technology, Visvesvaraya Technological University, Tumakuru, Karnataka, India

² Aircraft Research & Design Centre, HAL, Bangalore, Karnataka, India

³ School of Engineering, Presidency University, Bengaluru, Karnataka, India

and attributed that wear resistance increased because of the increase in ceramic particles. Surappa et al. [8] have reported that the addition of five vol% $\text{Al}_2\text{O}_{3\text{p}}$ increased the wear and tear characteristics of Al–Si mixtures. Bharath et al. [9, 10] have reported that at a constant speed and load, the wear rate of 6061Al– $\text{Al}_2\text{O}_{3\text{p}}$ decreased because of the increase in the sliding distance of 1500 m up to 12 wt% of ceramic particles. In particulate reinforced composites, usually vortex is created to bring the particles inside the alloy matrix during the stir technique. Most of the fabrication ways have utilised stir casting to make a vortex. The surviving negative pressure differential in the vortex sucks particles remotely in the liquid metal; the vortex additionally sucks in air bubbles which bring about extensive porosities in cast composites. Extensively, compo casting and liquid soften stirring are two types of manufacturing ways for creating composites with outwardly introducing particles; it depends on the temperature at which the particles are introduced into the melt. In both methods, due to the way vortex is employed, the porosities measure high [11], the above casting methods are most economical when used along with different techniques particularly powder metallurgy. Regardless of the approach that powder metallurgy delivers higher mechanical properties in MMCs, liquid state processing has some significant advantages, including improved matrix–particle interaction, low processing cost, simpler matrix structure regulation, flexibility, nearer to net-shaped form and size of the part and wide selection of materials [10]. On the other hand, the melting process has two major problems: first, the ceramic particles are usually not wetted by the liquid metal matrix, and second, the particles appear to float or sink in proportion to their liquid metal content. In order to enhance the properties, wettability is an important aspect. Wettability is overcome by pre-heating the reinforcement to expel absorbed gases, effective stirring and surface coating on the reinforcement [12]. The wear properties of the composites rely on the measurement, quantity, scattering and a sort of hard ceramic particles. Modification in mechanical and wear properties of the composites are due to the addition of ceramic particles nonetheless, diminish ductility. Therefore, looking at the wear and tear attributes of reinforced Al with ceramic particles is a remarkable space of analysis work. With this discourse, in the present work, endeavour is made to prepare 2014Al– $\text{Al}_2\text{O}_{3\text{p}}$ composites made by liquid stirring method and to find out the impact of $\text{Al}_2\text{O}_{3\text{p}}$ on

mechanical and wear result of the as-cast 2014Al alloy and composites with varying wt% of $\text{Al}_2\text{O}_{3\text{p}}$.

2 Experimental Procedure

2.1 Materials

In the present survey, 2014Al alloy/Al–Cu alloy is employed due to its high hardness and higher machinability, the chemical composition of 2014Al alloy is analysed with the assistance of Atomic Absorption spectroscopic analysis (Model AA-670, Varian, the Netherlands) and is shown in Table 1. The strength of the 2014Al alloy is due to coherency strains connected with ultimately fine copper-rich zones [13]. Al_2O_3 of an average particle size of 53 μm is used as strengthening material due to its superior strength and wear resistance properties. Composites were processed with 9, 12 and 15 wt% of Al_2O_3 particulates. The physical and mechanical properties of 2014Al alloy and $\text{Al}_2\text{O}_{3\text{p}}$ are presented in Table 2 [14].

2.2 Composite Preparation and Characterization

In the present examination, 2014Al– $\text{Al}_2\text{O}_{3\text{p}}$ composites were prepared by liquid stirring method. $\text{Al}_2\text{O}_{3\text{p}}$ particles with an average particle size of 53 μm were used as reinforcement. 2014Al (charge) is superheated to a temperature of 750 °C in a resistance furnace. Once the desired temperature is achieved, solid hexachloroethane (C_2Cl_6) is employed as degasser to get rid of the absorbed gases. At this stage, $\text{Al}_2\text{O}_{3\text{p}}$ preheated at 250 °C were added to the melt. Accurately measured amounts of $\text{Al}_2\text{O}_{3\text{p}}$ were added to melt. A unique two-stage combination is opted; reinforcement was divided into two halves rather than adding it once. During the introduction of ceramic Al_2O_3 particles, mechanical stirring is performed at a speed of 200 rpm for a period

Table 2 Physical and mechanical properties of 2014Al alloy and $\text{Al}_2\text{O}_{3\text{p}}$ [14]

Mechanical/ properties	Density (g/cm^3)	Hardness (HB500)	UTS (MPa)	Elastic modulus (GPa)
2014Al	2.8	135	483	70–80
$\text{Al}_2\text{O}_{3\text{p}}$	3.8	1175	665	300

Table 1 Showing the chemical composition of 2014Al alloy (by atomic absorption spectroscopic analysis—model AA-670, Varian, the Netherlands)

Elements (wt%)	Si	Fe	Cu	Mn	Mg	Cr	Zn	Ti	Others	Al
Al–Cu alloy	0.7	0.2	4.5	0.83	0.63	0.01	0.19	0.06	0.05	Rest

of 10 min utilizing zirconia-covered steel vane. Within the wake of guaranteeing higher dispersion of ceramic particles, a gushing temperature of 750 °C is opted and also the liquefied melt is introduced into the forged iron mould.

Central parts of the casted specimen were cut and polished by using grit papers and diamond paste; SEM images were taken by using scanning electron microscope (SEM). Micro hardness and tensile test results were measured by using Zwick indenter digital microhardness tester and UTM as per ASTM E92-17 and ASTM E-8 standards. The wear tests were conducted as per ASTM-G99 standards on clean pin made from composites having a dimension of 8 mm diameter and 30 mm length against a rotating disc made from steel with a track diameter of 80 mm. The initial weight of the specimens was weighed using an electronic weighing machine with a precision of 0.0001 g. The counter facial disc was cleaned with acetone after each test. Before and after testing, the pin was weighed to determine the amount of wear loss. At room temperature, wear rate is calculated as a part of sliding distance and load. Tests were conducted for each synthesized composite at a constant speed of 300 rpm

and at a constant load of 29.43 N. Additionally, to work out the wear mechanism, worn surfaces were examined by SEM.

3 Results and Discussions

3.1 Characterization of the Prepared Composites

Microstructural investigations were done on the synthesized composites with the assistance of SEM to see the uniform distribution of hard ceramic Al_2O_3 in 2014Al alloy matrix. Figure 1a–d demonstrate the SEM images of as-cast 2014Al alloy and 2014Al alloy combination with 9, 12 and 15 wt% Al_2O_3 . The microstructure comprises of essential α -Al dendrites and eutectic copper as shown in Fig. 1a, whereas Al_2O_3 particles are found in between dendritic regions also in the mixture of copper. Figure 1b–d exhibit the SEM images of the composite with different weight percentage of Al_2O_3 from 9 to 15 wt%.

For above synthesized composites, Fig. 1b–d indicate uniform dispersion of Al_2O_3 . The uniform distribution of

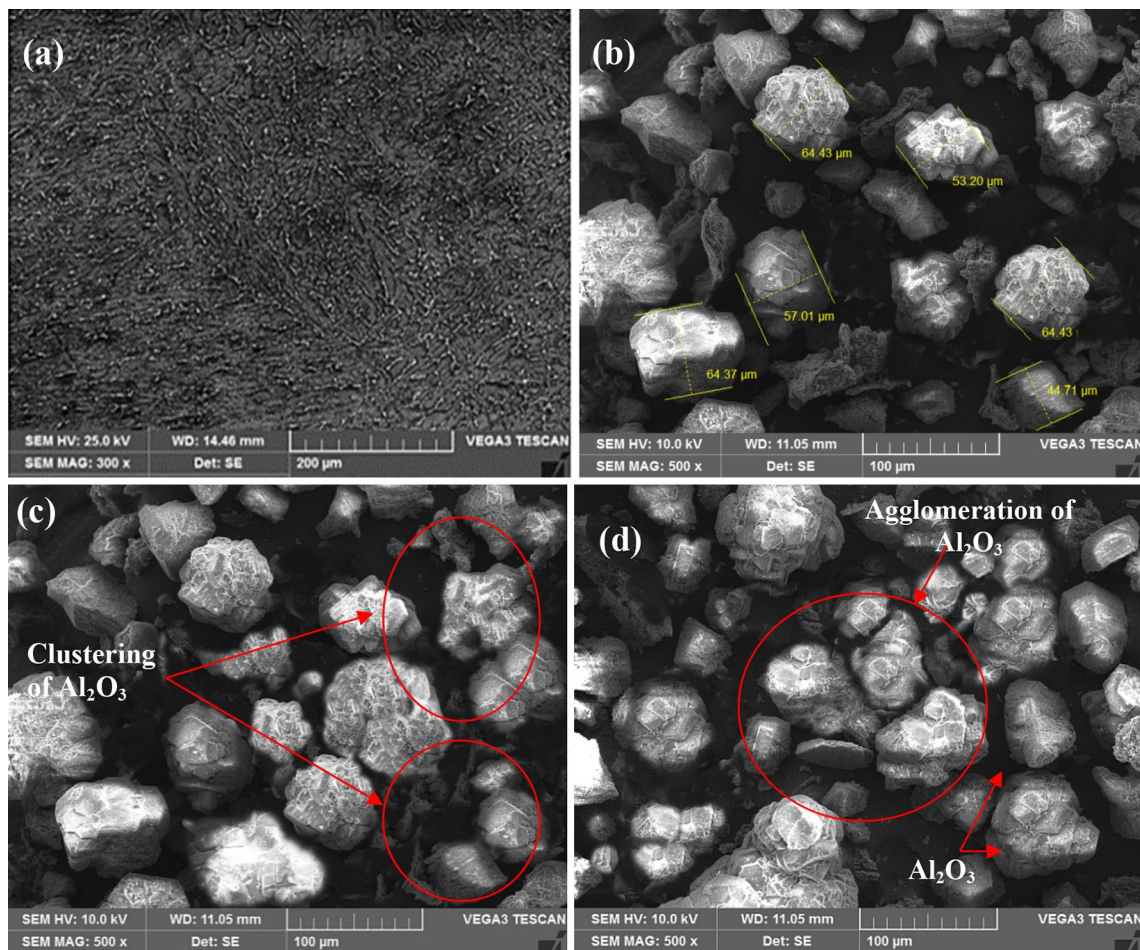


Fig. 1 a–d SEM images of a 2014Al alloy, b 2014Al–9 wt% Al_2O_3 , c 2014Al–12 wt% Al_2O_3 and d 2014Al–15 wt% Al_2O_3

strengthening particles obtained in the synthesized composite is the end result of 2-stage stirring. In view of the fact that the whole weight of the reinforcing particles is added in 2-steps which ensure uniform dispersion overcome the viscosity divergence. As revealed in Fig. 1b–d, homogeneous dispersion of the Al_2O_3 was accomplished in the composites reinforced with $53\ \mu\text{m}$ Al_2O_3 . Figure 1a shows the SEM images of cast matrix of 2014Al and Fig. 1c and d reveal the SEM images of the clustering and agglomeration of 12 and 15 wt% of Al_2O_3 , probably owing to the fact that with increase in wt% of reinforcement, there is a possibility of forming destabilized bond between matrix and reinforcement which result in increase of surface energy and thereby decreasing the wettability [15, 16].

3.2 Energy-Dispersive X-Ray Spectroscopy (EDS) and XRD

Figure 2 demonstrates EDS of surface of the 2014Al–12 wt% Al_2O_3 composite specimen which signifies the existence of Oxide (O) in the 2014Al alloy matrix thereby confirming the presence of Al_2O_3 particles.

For the 2014Al–12 wt% Al_2O_3 composite, XRD analysis was performed to confirm the presence of Al_2O_3 and the outcomes are shown in Fig. 3. The peaks obtained from the X-Ray diffraction of the above synthesized composite sample are contrasted with data from JCPDS (Joint Commission for Powder Diffraction Standards). From the Fig. 3, the peaks of Al_2O_3 at 43.732° , 53.026° , 58.049° and 77.715° (JCPDS File No. 75-0787) and peaks of pure Al at 38.44° , 44.7° , 65.32° and 77.2° are identified in the prepared composites with other minor impurity peaks.

3.3 Microhardness

Figure 4 is the evidence for the consequences of micro Vickers hardness tests performed on 2014Al alloy and furthermore on the 2014Al composite containing different weight proportions (9, 12 and 15 wt%) of Al_2O_3 particles. The Micro Vickers hardness was estimated on the prepared samples by the use of precious stone cone indenter with a load of 20 N and the value is noted down with an average of hundred readings taken at different spots. Figure 4 presents micro hardness estimates for various weight proportions of reinforcement. It indicates that the hardness values of composite reinforced with different weight proportions of Al_2O_3 is higher than the cast matrix 2014Al alloy. In case of cast matrix 2014Al alloy, the hardness value was 99.23 VHN. Composites reinforced with Al_2O_3 at 9, 12 and 15 wt% reveal hardness values to be 127.89, 142.26 and 167.25 VHN, respectively, whereas composites containing a maximum weight percentage (15 wt%) of Al_2O_3 show the most elevated hardness (167.25 VHN). The most extreme observed increment in hardness of composites when contrasted with unreinforced 2014Al alloy was found to be 68.54%. The essential growth for increment in hardness of the matrix is because of the nearness of Al_2O_3 [17]. Reinforcing particles are harder and stiffer than matrix, which builds limitation to plastic distortion of matrix throughout the experiment [10]. Increase in weight proportion of reinforcement results in increase in hardness because of valid appropriation of Al_2O_3 particles. It might likewise be noticed that hardness pattern acquired in the present investigation is like the discoveries detailed for ceramic-reinforced 6061Al matrices in the micrometre length scale of the reinforcement [10].

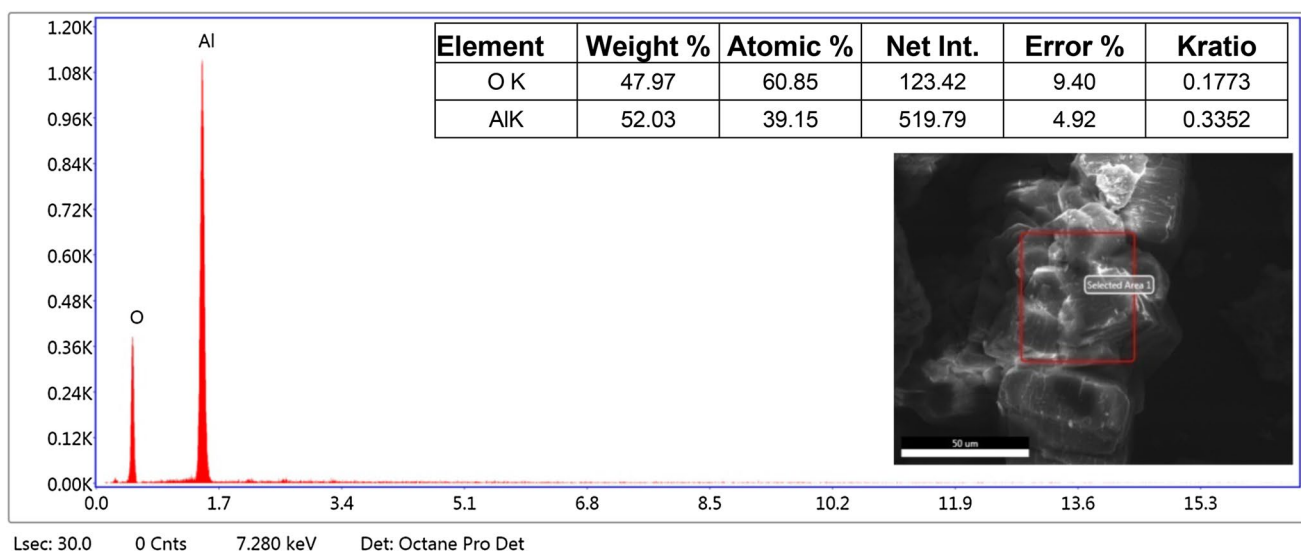


Fig. 2 EDS outcomes of 2014Al–12 wt% Al_2O_3 composite

Fig. 3 XRD pattern of 2014Al + 12 wt% Al_2O_3 composite

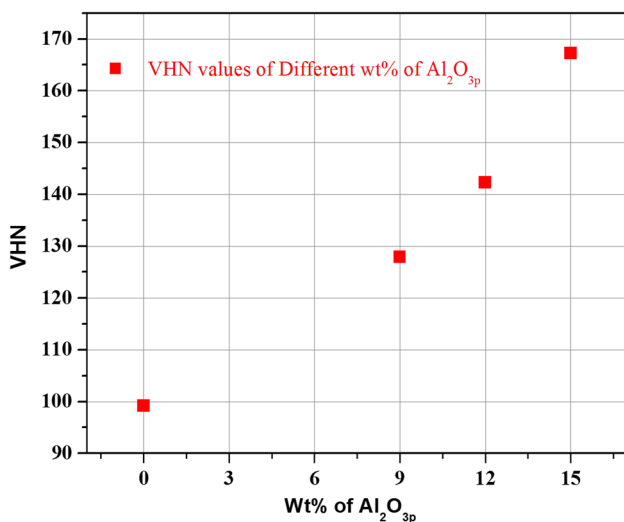
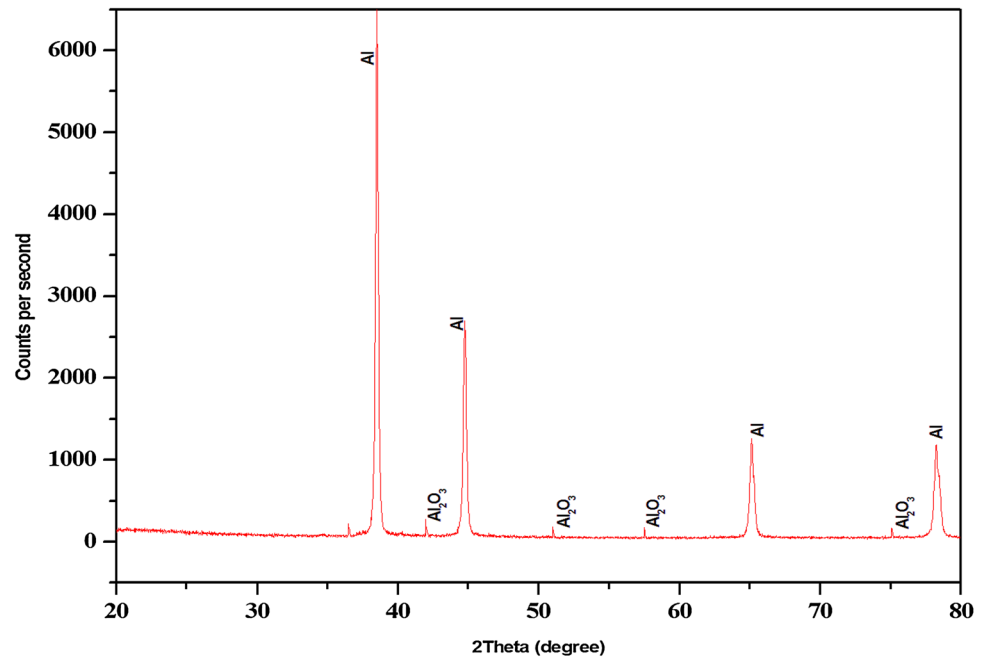


Fig. 4 Micro Vickers Hardness of 2014Al alloy prior and after adding up of different wt% (9, 12, and 15 wt%) of Al_2O_3 particulates

3.4 Tensile Test

The objective of tensile testing is to characterize the mechanical behaviour of the prepared composites under tensile loading. A strong internal stress is created utilizing malleable loads which can result in confined breakdown when the nearby stress surpassed the material strength. The uniform dispersion of reinforcement particles facilitates the spread of stress and prevents the development of localized damage [18]. Figure 5 demonstrates the distinction of tensile and yield strength of cast matrix 2014Al

alloy and the composite. The value of tensile strength of cast matrix 2014Al was found to be 175.73 MPa. The increase in Al_2O_3 reinforcement content by 9, 12 and 15 wt% of the composite revealed tensile strengths of 175.73, 184.69 and 226.75 MPa. Unmistakable rigidity of composites is more prominent when contrasted with as-cast 2014Al.

It may very well be seen that the weight percentage of the Al_2O_3 expands the distribution of stress to hard phase, which thusly builds the elasticity. The clarifications behind improvements gained with Ultimate Tensile Strength (UTS) are (i) extreme hardness at the interface between the ceramic particle and base metal bond dependent on load movement [19]; (ii) changes in the microstructure throughout the treatment of composites, in light of the exchange of the load between the hard ceramic Al_2O_3 and ductile matrix 2014Al alloy bringing about fortifying and overhauling rigidity [19, 20]. The Yield strength of the synthesized composites is observed to increase with the increase in weight proportion of hard ceramic Al_2O_3 in 2014Al composites. The strength of the synthesized composites consistently depends on the size of the particles between the matrix and the reinforcement and interfacial bond [21].

On the off chance that the matrix-reinforcement bond is adequate, the stress applied can be moved from the soft matrix to the hard Al_2O_3 at that point. The higher strength due to the presence of Al_2O_3 particles secures the matrix of the moderately soft alloy. The yield strength of the base material (0.2% offset) is 169.76 MPa, whereas the highest yield strength measured is 194.93 MPa for a 15% weight fraction (Fig. 5).

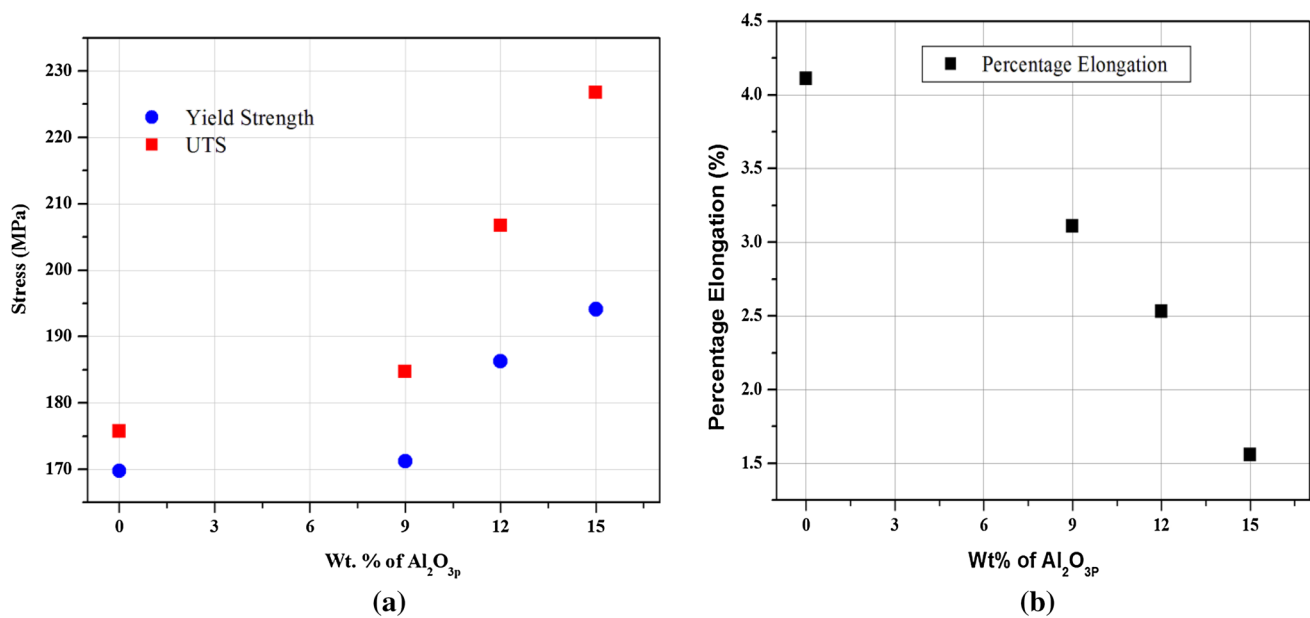


Fig. 5 Variation of **a** yield and tensile strength with different wt% of Al_2O_{3p} , **b** percentage of elongation with different wt% of Al_2O_{3p}

With a rise in weight fraction level, it is possible to move more loads to the reinforcement, which also contributes to better yield strength [18]. The pliability of the 2014Al alloy composite is affected by the strengthening. As shown in Fig. 5b, the percentage of elongation varies from 4.11% for 2014Al alloy to 1.56% for 2014Al alloy with 15% weight fraction of Al_2O_{3p} . Due to void nucleation, the decrease in ductility can be credited with increasing reinforcement measure. The high stress concentration at the tip of the broken particles can also help to reduce the composite ductility. The precise cause for this dissimilarity may be the way alumina particles behave as stress concentration agents. This job is made easier by the agglomeration of particles. Thus, the extent of stress increases during tensile loading significantly, closes to the agglomerated micro particles and makes the matrix and reinforcement de-bonding between the reinforcement and matrix [22].

3.5 Wear Study

For the wear study, a wear track of diameter 80 mm and a load of 29.43 N was set for all the measurements, with the sliding speed of 300 rpm. Figure 6a and b demonstrate the effects of weight loss and wear rate as a sliding distance feature performed on 2014Al–9, 12 and 15 wt% Al_2O_{3p} . Figure 6a demonstrates the utmost weight loss in 2014Al compound and minimum weight loss in 2014Al–15 wt% Al_2O_{3p} . The wear loss of the cast matrix 2014Al alloy is higher than those of composites reinforced by Al_2O_{3p} [23]. The increased wear loss in 2014Al alloy

is due to delamination in the alloy where fragments are moved from the pin to the disc and larger fragments are thrown out. The implementation of the 2014Al– Al_2O_{3p} step eliminates the loss of wear. Al_2O_{3p} provides enhanced wear resistance to the Al composites as compared to cast matrix 2014Al alloy by forming mechanically mixed layers at the composite specimen and steel disc interface.

Figure 6b demonstrates the wear rate of 2014Al and Al_2O_{3p} -reinforced composites. Generally, the wear loss in terms of weight loss or height loss is more as sliding distance increases from 600 to 3600 m. In the present investigations, wear rate is calculated by load and sliding distance dividing the volumetric wear loss; as denominator component sliding distance increases from 600 to 3600 m, the wear rate is decreased. As discussed earlier, here also, wear rate is more in unreinforced alloy 2014Al. As percentage of Al_2O_{3p} increases from 9 to 15 wt% in steps of 3 wt%, the wear rate decreases. The decrease in wear rate and increase in wear resistance in composites is due to the presence of Al_2O_{3p} phase that acts as load-supporting element. Also, the presence of reinforcement phase on the sliding surface effectively covers the 2014Al matrix alloy and is attributed to the high hardness of Al_2O_{3p} -reinforced composites which also helps to improve the wear resistance [24]. The Al_2O_{3p} reinforcement process within the 2014Al matrix avoids the steel counterpart ploughing operation and improves the wear resistance [9]. The wear protection of the composites considerably increased as a result of introduction of the Al_2O_{3p} and increases with increasing Al_2O_{3p} wt%.

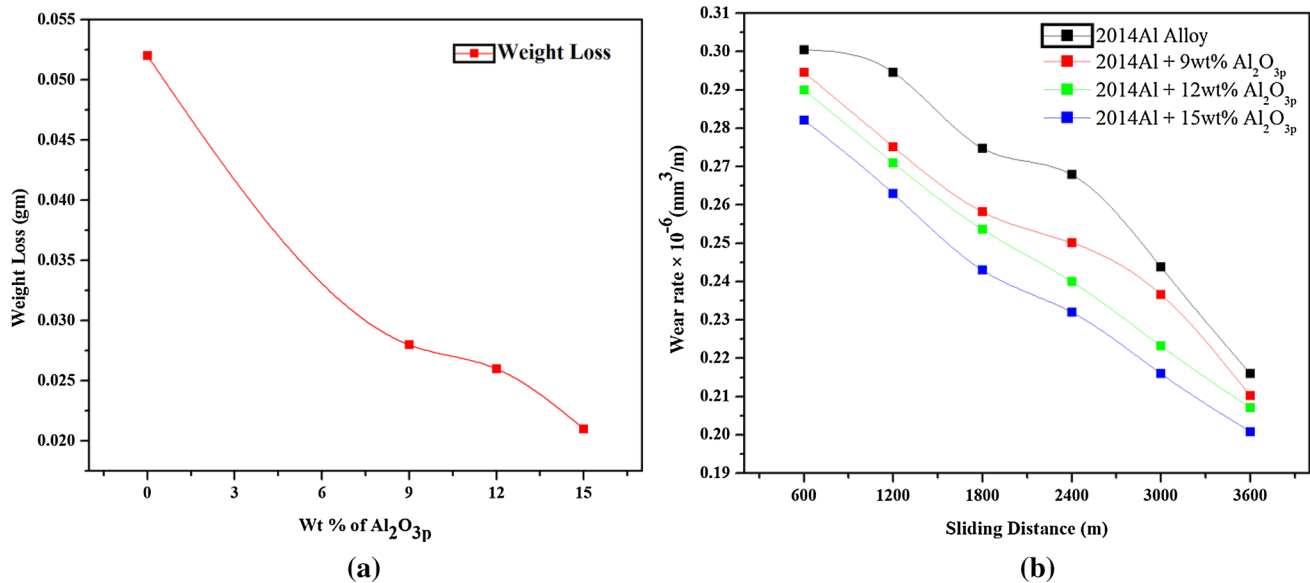


Fig. 6 **a** Weight loss as a function of Al₂O_{3p} wt% and **b** wear rate of alloy and composites as a function of sliding distance

3.6 Worn Surface Studies of the Prepared Composites

Study of worn surfaces of 2014Al alloy and 2014Al–Al₂O_{3p} composites were examined through a scanning electron microscope. Figure 7a–h demonstrate the SEM images of worn surfaces of 2014Al alloy and 2014Al–Al₂O_{3p} composites of various wt% (9, 12 and 15 wt%) at a load of 29.43 N, sliding speed of 300 rpm and sliding distance of 3600 m. In the current research, optimum values have been used to conduct wear studies. If the applied normal load and sliding speed is too low, it is difficult to analyse the wear behaviour of alloy and composites. Further, if the applied load and speed are high, the material loss is more and sometimes causes the seizure of pin material along with disc. Hence, in the present research, moderate load and speeds have been used to evaluate the wear behaviour. Usually, the loss of the material is more during initial sliding distance, and as the sliding distance further increases beyond a certain value the material loss will be less; hence a numerical distance of 3600 m is used in the present research. The base alloy SEM photos show that a higher amount of material throughout the study has been excluded from the surface of the pin.

From Fig. 7a and b, shallow wear tracks and surface delaminations are very evident. In sliding wear test, in light of the fact that the unreinforced composite was extensively softer than the slider, the slider may enter and cut considerably into the surface, inflicting plastic surface deformation and thus showing excessive material loss [7]. Figure 7a and b of as-cast shows that shallow wear tracks and surface delamination are obvious. Wear path shows the mechanism of abrasive wear; surface delamination found at scattered

locations often leads to a substantial wear rate. Adding Al₂O_{3p} to the 2014Al matrix resulted in lower wear rates compared to the 2014Al wear rates alone as evident from the worn surface images, Fig. 7c–h. It is observed from Fig. 7f and h that some cracks are formed at the aluminium grain boundaries. This could be attributed to the pressure hardening [5] of aluminium during sliding with an applied load and the pulling up of hard phase particles and these cracks formed parallel to the sliding path as shown in Fig. 7d and h. The wear and tear track was secured with a defensive chemical compound layer confirming the reduction of wear and tear rate at the sliding distance of 3600 m as shown in Fig. 7h. Development of those tribolayers can be the first rationalization behind the decreasing wear rate of composites [25]. The Al₂O_{3p} discharged on the wear and tear surface throughout the wear and tear method avoids direct metal-to-metal contact and acted as a lubricator, thus, reducing the friction constant between the composite pin and the steel disc [24].

Examination of worn surfaces showed that the worn surface of the composite alloy is generally much rougher than that of the alloy as shown in Fig. 7a and b. In addition, the abrasive wear process (Fig. 7g–h) is found in the 2014 Alloy-reinforced Al₂O_{3p} composites, which is primarily the result of rough Al₂O_{3p} applied to worn surfaces and loose fragments between two materials. Considering that the Al₂O_{3p} avoids the cycle of the delamination, the wear resistance of the 2014Al alloy-reinforced Al₂O_{3p} composites is more in case. Within the wear testing conditions, the principal mechanism is small, cutting and ploughing is for the composites containing tiny particles, whereas it is crushing for the composites containing massive particles [7]. During

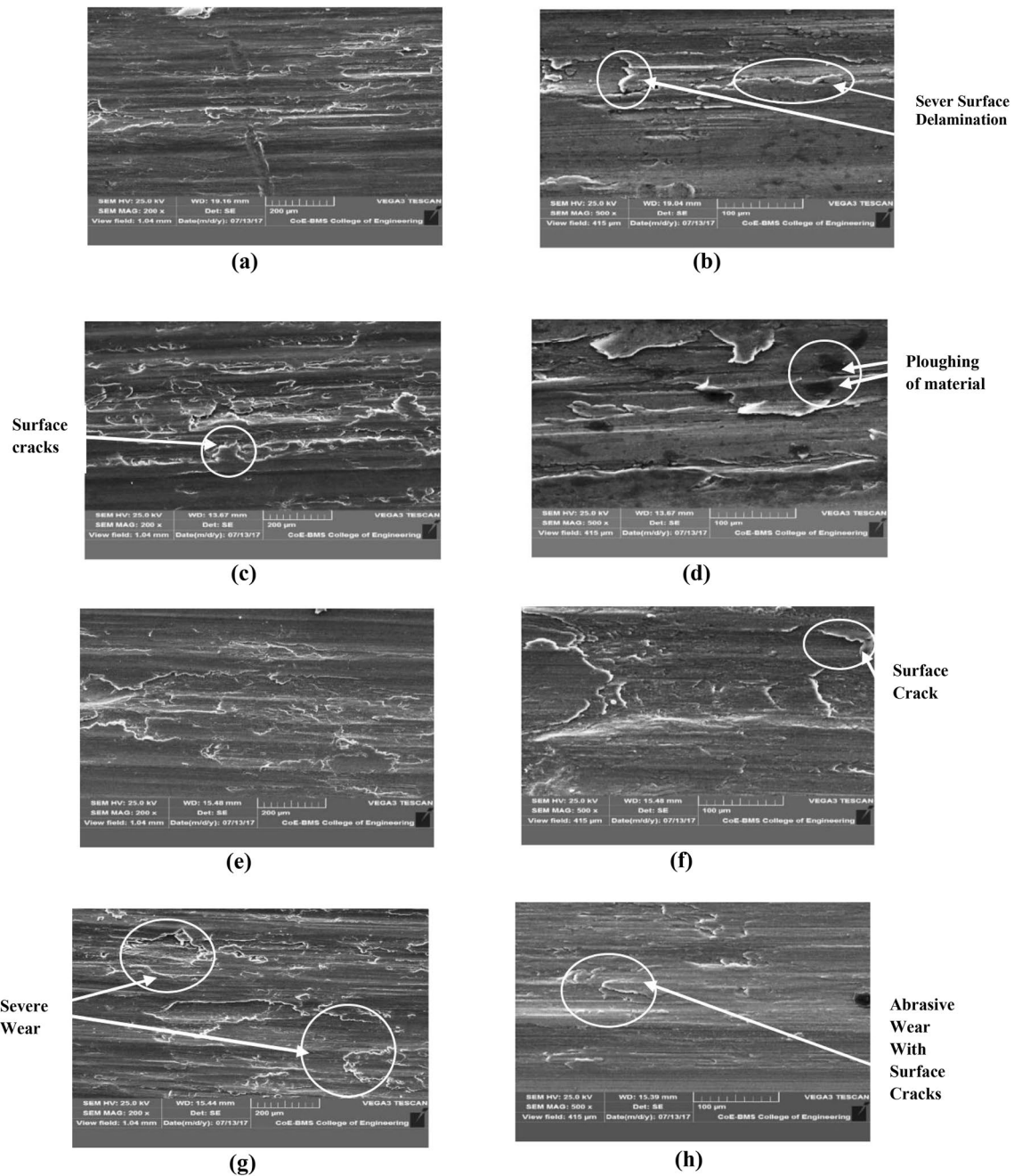


Fig. 7 Scanning electron micrographs of **a, b** 2014Al alloy, **c, d** 2014Al+9 wt% $\text{Al}_2\text{O}_3\text{p}$, **e, f** 2014Al+12 wt% $\text{Al}_2\text{O}_3\text{p}$ and **g, h** 2014Al+15 wt% of $\text{Al}_2\text{O}_3\text{p}$ composite

the wear, the oxidized surface acts as barrier for the material loss and reduces the wear (Fig. 7c–h). Moreover, the compaction and fragmentation of this wear scrap counter surface material and thin chemical compound layers incite the arrangement of an automatically mixed layer that shields the specimen surface from wear. Further, increasing sliding distance prompts to increase the temperature that makes the subsurface to soften because of plastic deformation and formation of MML (mechanically mixed layer) that takes

place on the pin surface. Thus, at longer sliding distances, it is typical that the formation and removal of MML occurs at an equivalent time and also the rate of removal and development of MML can be similar, and thus, the wear rate stay unchanged with sliding distance [5, 26].

EDS examination of the worn surface is shown in Fig. 8; the first perception is the measure of iron present within the surface (Fig. 8). Iron is transferred from the worn counter face through a mechanical alloy process that results in the

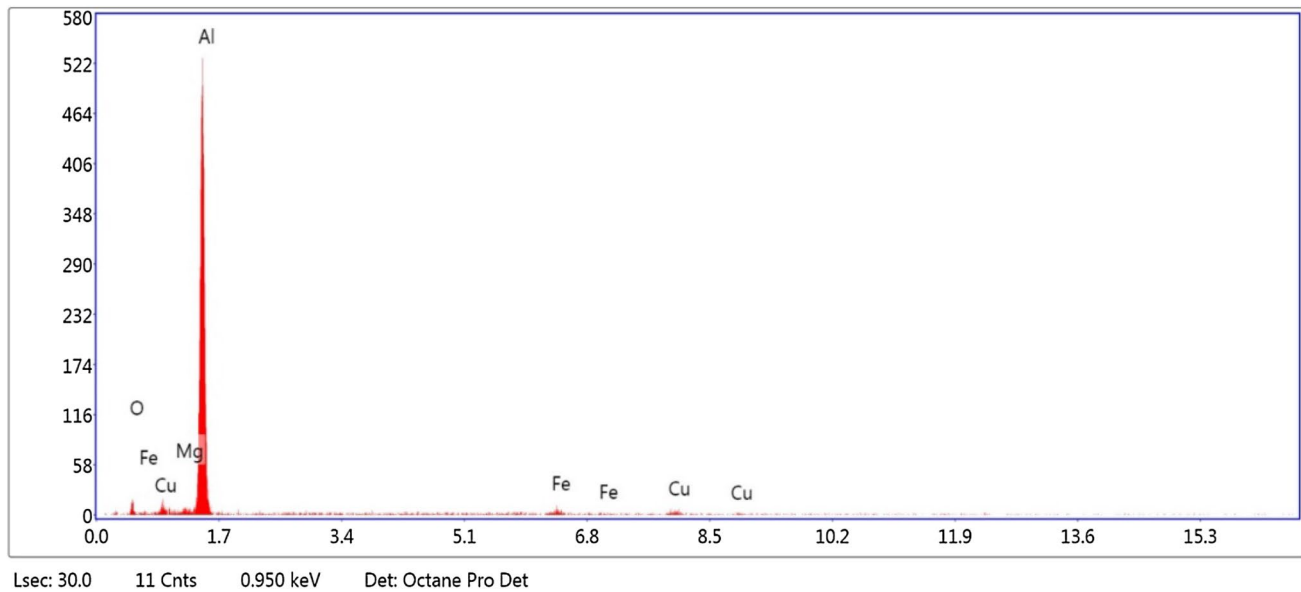


Fig. 8 EDS analysis of worn surface of 2014Al–15wt% Al₂O_{3p}

wearing surface becoming an MML. This shows that the transition layer of iron prevents interaction between surfaces and thus increases wear resistance [27]. This conduct is in strong consonance with Rosenberger et al.' s results [28].

4 Conclusions

The current study on 2014Al alloy reinforced with different weight proportions (9, 12 and 15 wt%) of Al₂O_{3p} has led to the subsequent conclusions.

1. 2014Al–Al₂O_{3p} metal matrix composites are effectively synthesized with different weight percentages using a liquid stirring technique.
2. The SEM images of liquid stirring technique composites display a fairly uniform distribution of Al₂O_{3p} in the 2014 Al MMC's with less agglomeration.
3. Improvements in hardness of 28.88, 43.36 and 68.54 percent were achieved by adding 9, 12 and 15 wt% of Al₂O_{3p}, respectively, compared to the 2014 Al matrix. With an improvement of 68.54 percent micro hardness, the 15 wt% of Al₂O₃-reinforced 2014Al composite has good mechanical properties compared to other reinforcements reported. However, the composite hardness increases with increasing Al₂O_{3p} weight percentage.
4. Minimum wear rate was ascertained for 2014Al that is strengthened with 15 wt% of Al₂O_{3p} at a continuing load of 29.43 N, sliding speed of 300 rpm and sliding distance of 3600 m as compared to the base alloy.

5. Formation of protecting compound layer at an intermediate slippery distance of 3600 m was ascertained and that confirms the minimum wear rate of the composite and are discernible from the worn surface microphotographs.

Compliance with Ethical Standards

Conflict of interest On behalf of all authors, the corresponding author states that there is no conflict of interest.

References

1. Alpas AT, Zhang J (1994) Effect of microstructure (particulate size and volume fraction) and counter face material on the sliding wear resistance of particulate-reinforced aluminum matrix composites. *Metall Mater Trans A* 25A:969–983. <https://doi.org/10.1007/BF02652272>
2. Alpas AT, Embury JD (1990) Sliding and abrasive wear behaviour of aluminum (2014)-sic particle reinforced composite. *Scr Metall Mater* 24:931–935. [https://doi.org/10.1016/0956-716X\(90\)90140-C](https://doi.org/10.1016/0956-716X(90)90140-C)
3. DanielJebin V, Shivalingappa D, Jenix Rino J (2013) Wear behavior of AL6063-alumina metal matrix composite. *Int J Sci Res* 2:446–449
4. Rajesh AM, Kaleemulla M (2016) Experimental investigations on mechanical behavior of aluminium metal matrix composites. *Mater Sci Eng* 149:1–12. <https://doi.org/10.1088/1757-899X/149/1/012121>
5. Roa RN, Das S (2011) Effect of sliding distance on the wear and friction behavior of as cast and heat-treated-SiCp composites. *Mater Des* 32:3051–3058. <https://doi.org/10.1016/j.matdes.2011.01.033>

6. Hassan AM, Alrashdan A, Hayajneh MT, Mayyas AT (2009) Wear behavior of Al–Mg–Cu–based composites containing SiC particles. *Tribol Int* 42:1230–1238. <https://doi.org/10.1016/j.triboint.2009.04.030>
7. Kok M, Ozdin K (2007) Wear resistance of aluminium alloy and its composites reinforced by Al₂O₃ particles. *J Mater Process Technol* 183:301–309. <https://doi.org/10.1016/j.jmatprotec.2006.10.021>
8. Surappa MK, Prasad SV, Rohatgi PK (1982) Wear and abrasion of cast Al–Alumina particle composites. *Wear* 77:295–302. [https://doi.org/10.1016/0043-1648\(82\)90055-2](https://doi.org/10.1016/0043-1648(82)90055-2)
9. Bharath V, Nagaral M, Auradi V, Kori SA (2014) Studies on dry sliding wear characteristics of ceramic Al₂O₃ particulate reinforced 6061Al matrix composites. *Adv Mater Res* 985:319–325. <https://doi.org/10.4028/www.scientific.net/AMR984-985.319>
10. Bharath V, Nagaral M, Auradi V, Kori SA (2014) Preparation of 6061Al–Al₂O₃ MMCs by stir casting and evaluation of mechanical and wear properties. *Procedia Mater Sci* 6:1658–1667. <https://doi.org/10.1016/j.mspro.2014.07.151>
11. Yilmaz O, Buytoz S (2001) Abrasive wear of Al₂O₃-reinforced aluminium-based MMCs Composites. *Sci Technol* 61:2381–2392. [https://doi.org/10.1016/S0266-3538\(01\)00131-2](https://doi.org/10.1016/S0266-3538(01)00131-2)
12. Mithun BR, Nagaral M, Auradi V, Bharath V (2017) Microstructure and mechanical properties of Cu-coated Al₂O₃ particulate reinforced 6061 Al metal matrix composite. *Mater Today* 4:11015–11022. <https://doi.org/10.1016/j.matpr.2017.08.060>
13. Bhansali KJ, Mehrabian R (1982) Abrasive wear of aluminum-matrix composites. *J Metals*. <https://doi.org/10.1007/BF03338093>
14. ASM Handbook (1990) ASM handbook Committee, pp 62–122. <https://doi.org/10.1361/asmhba0001060>
15. Kok M (2004) Production and mechanical properties of Al₂O₃ particle-reinforced 2024 aluminium alloy composites. *J Mater Process Technol* 161–3:381–387. <https://doi.org/10.1016/j.jmatprotec.2004.07.068>
16. Chaudhary SP, Singh PK, Rai S, Patel H, Kumar B (2015) A review on effect of reinforcement particles on the mechanical properties of aluminium based composites. *Int J Innov Res Sci Eng Technol* 4(9):8377–8382
17. Mittal P, Dixit G (2016) Dry sliding wear behaviour of 2014 aluminium alloy reinforced with SiC composite. *Int J Eng Res Technol* 5:147–153
18. Aravindan S, Rao PV, Ponappa K (2015) Evaluation of physical and mechanical properties of AZ91D/SiC composites by two step stir casting process. *J Magnes Alloys* 3:52–62. <https://doi.org/10.1016/j.jma.2014.12.008>
19. Gaharwar VS, Umashankar V (2014) The characterization and behavior of Al2014 reinforced with Al₂O₃ fabricated by powder metallurgy. *Int J Chem Technol Res* 6:3272–3275
20. Modi OP (2001) Two-body abrasion of a cast Al–Cu (2014Al) alloy–Al₂O₃ particle composite: influence of heat treatment and abrasion test parameters. *Wear* 248:100–111. [https://doi.org/10.1016/S0043-1648\(00\)00534-2](https://doi.org/10.1016/S0043-1648(00)00534-2)
21. Casati R, Vedani M (2014) Metal matrix composites reinforced by nano-particles—a review. *Metals* 4:65–83. <https://doi.org/10.3390/met4010065>
22. Sajjadi SA, Ezatpour HR, Beygi H (2011) Microstructure and mechanical properties of Al–Al₂O₃ micro and nano composites fabricated by stir casting. *Mater Sci Eng A*. <https://doi.org/10.1016/j.msea.2011.08.052>
23. Mallikarjun B, Shashidhar SM, Mallik US, Parashivamurthy KI (2011) Grain refinement and wear properties evaluation of aluminum alloy 2014 matrix–TiB₂ in-situ composites. *Mater Des* 32:3554–3559. <https://doi.org/10.1016/j.matdes.2011.01.036>
24. Babu JSS, Kang CG, Kim HH (2011) Dry sliding wear behavior of aluminum based hybrid composites with graphite nano fiber–alumina fiber. *Mater Des* 32:3920–3925. <https://doi.org/10.1016/j.matdes.2011.02.064>
25. Abedini M, Ghasemi HM, NiliAhmadabadi M (2012) Effect of normal load and sliding distance on the wear behavior of NiTi alloy. *Tribol Trans* 55:677–684. <https://doi.org/10.1080/10402004.2012.688166>
26. Korkut HM (2004) Effect of particulate reinforcement on wear behavior of aluminium matrix composites. *Mater Sci Technol* 20:73–81. <https://doi.org/10.1179/174328413X13789824293542>
27. Baradeswaran A, Elaya Perumal A (2014) Study on mechanical and wear properties of Al 7075/Al₂O₃/graphite hybrid. *Composites B* 56:464–471. <https://doi.org/10.1016/j.compositesb.2013.08.013>
28. Rosenberger MR, Schvezov CE, Forlerer E (2005) Wear of aluminium matrix composites under conditions that generate a mechanically mixed layer. *Wear* 259:590–601. <https://doi.org/10.1016/j.wear.2005.02.003>

Publisher's Note Springer Nature remains neutral with regard to jurisdictional claims in published maps and institutional affiliations.